Supporting Information

Reconstruction of ZIF-67 Structure and Boosted Hydrogen Evolution Reaction in Alkaline Medium

Hanghang Guo[a], Aibing Chen[a,], Wanliang Mi[c], Suojiang Zhang[b], Yajuan Zhang[b], Xingwei Shi[b,*]*

[a] College of Chemical and Pharmaceutical Engineering, Hebei University of Science and Technology, 26 Yuxiang Street, Shijiazhuang, 050018, China. E-mail: chen_ab@163.com

[b] Institute of Process Engineering, Chinese Academy of Sciences, Beijing, 100190, China. E-mail: xwshi@ipe.ac.cn

[c] State Key Laboratory of Catalytic Materials and Reaction Engineering (RIPP, SINOPEC)

Experimental section

1. Materials

Cobalt nitrate hexahydrate ($Co(NO_3)_2{\cdot}6H_2O$, AR), hydrochloric acid (HCl, AR), acetone (CH_3COCH_3, AR) and potassium hydroxide (KOH, AR) were purchased from Sinopharm Chemical Reagent Co., Ltd. Cobalt sulfate heptahydrate ($CoSO_4{\cdot}7H_2O$, AR, ≥99%), sodium succinate ($C_4H_4Na_2O_4$, AR, 99%) and dimethylamine borane (DMAB, Et_2NHBH_3, 96%) were purchased from Aladdin. 2-Methylimidazole ($C_4H_6N_2$, 98%), Pt-C (20% Pt), sodium sulfate anhydrous (Na_2SO_4, AR, 99%) and sodium hypophosphite monohydrate ($NaH_2PO_2{\cdot}H_2O$, AR) were

purchased from Shanghai Macklin Biochemical Technology Co., Ltd. Anhydrous methanol was purchased from Tianjin Damao Chemical Reagent Factory. Ethanol (C_2H_6O, AR) was purchased from Xilong Chemical Co., Ltd. Ni foam (NF) was purchased from Changde Liyuan New Materials Co., Ltd. The water used in this experiment is deionized water. The chemicals used in an experiment or analysis were used in their as-received state, without undergoing any additional purification steps to remove impurities or enhance their purity.

2. Material synthesis

The EP bath for the CoB catalyst was prepared by dissolving Na_2SO_4 (1.5 g), sodium succinate (2.5 g) and $CoSO_4$ (1.38 g) in 100 mL water followed by the addition of DMAB (0.72 g) into the solution. The EP bath for the CoP catalyst was prepared by dissolving Na_2SO_4 (1.5 g), sodium succinate (2.5 g), $NaH_2PO_2 \cdot H_2O$ (0.094 g) and $CoSO_4$ (1.38 g) in 100 mL water.

Preparation of Pt-C/NF: 10 mg of 20 wt% Pt-C catalyst was added into 500 μL water, 485 μL ethanol and 15 μL Nafion solution. Ultrasonic treatment made the catalyst disperse evenly. Then, 10 μL of the mixture was dropped onto the nickel foam and dried under an ultraviolet lamp. The previous step was repeated until the catalyst load reached 9.4 mg cm^{-2}.

3. Structural characterization

Field-emission scanning electron microscopy (FESEM) measurements were performed on a Gemini 300 field at an accelerating voltage of 2 kV. Transmission electron microscope (TEM) measurements were carried out on a JEM-F200

microscope (JEOL, Japan) operated at 200 kV. Energy dispersive X-ray spectrometer (EDX) is a technique used to obtain the elemental composition and distribution of a sample. In this case, EDX mapping was characterized by HAADF-STEM. X-ray diffraction (XRD) was performed on a Rigaku D/MAX 2550 diffractometer with Cu Kα radiation (λ = 0.15406 nm). The X-ray photoelectron spectra (XPS) of the products were recorded using a Thermg ScientificK-Alpha with an Al Kα source. The Co, P, and B content of the materials were measured using the ICP-OES (Inductively Coupled Plasma Optical Emission Spectrometer) technique with an Agilent 5110 instrument.

4. Electrochemical measurements

The CHI 760E electrochemical workstation from Shanghai Chenhua was used to analyze the electrochemical properties of the samples. The experiment was conducted using a three-electrode system in which the prepared catalyst was used as the working electrode, the graphite rod was used as the counter electrode, and the Hg/HgO electrode was used as the reference electrode. In this paper, 1 M KOH solution was used as the electrolyte for electrochemical test. In addition, 85% iR-compensation was applied to the working electrode's performance. This compensation helps to account for the ohmic voltage reduction that can occur between the working electrode and the reference electrode. All applied potentials were converted relative to the reversible hydrogen electrode (RHE), $E_{RHE} = E_{Hg/HgO} + 0.059\ pH + 0.098\ V$. The polarization curves were obtained by linear sweep voltammetry (LSV) at a sweep rate of 5 mV s^{-1}. The Tafel equation ($\eta = b\ log\ |j| + a$) was then used to calculate the corresponding

Tafel curves from the polarization curves. The Tafel equation relates the overpotential (η) to the current density (j) and the Tafel slope (b). The interface charge transfer resistance was measured using electrochemical impedance spectroscopy (EIS) over a frequency range of 0.01-10^5 Hz. EIS is a technique that measures the impedance of an electrochemical system as a function of frequency. By analyzing the impedance data, it is possible to obtain information about the charge transfer resistance at the electrode-electrolyte interface. The double-layer capacitance (Cdl) of an electrochemical system, which is related to its electrochemically active surface area (ECSA). Cyclic voltammogram curves were collected at scan rates of 20, 40, 60, 80, and 100 mV/s in the potential range of 0.114-0.214 V vs RHE. The resulting data can be analyzed to determine C_{dl} and ECSA for the electrochemical system under study.

5 Turnover frequency (TOF)

The C_{dl} of HER for CoPB@ZIF-67/NF, CoPB/NF and ZIF-67/NF were determined to be 15.76 mF cm^{-2}, 10.23 mF cm^{-2} and 4.68 mF cm^{-2}, respectively (Fig. 3d). We assumed that the total number of surface sites, including cobalt, phosphide, and boron atoms, represented the number of active sites. Then, it is converted into a normalized turnover frequency (TOF) diagram based on current density. The double layer capacitance of the standard electrode (nickel foil) is about 60 μF $cm^{-2,}$ and the number of active sites on the surface is 1.164×10^{15}.

CoPB@ZIF-67/NF catalyst:

$$\text{RF CoPB@ZIF-67/NF} = \frac{C\ CoPB@ZIF-67/NF}{C\ dl\ Flat\ standard} = \frac{15.76\ mF\ cm-2}{60\ \mu F\ cm-2} = 262.7$$

The number (N) of surface-active sites per cm^{-2} is calculated based on,

$N_{NFs} = RF_{NFs} \times N_{Flat\ standard} = 262.7 \times 1.164 \times 10^{15} = 3.06 \times 10^{17}$

Then the per-site TOF is calculated by the following equation:

$$\text{TOF per site} = \frac{the\ number\ of\ total\ hydrogen\ turn\ overs}{the\ number\ of\ surface\ active\ sites}$$

The number of total hydrogen is calculated from the current density using the following equation:

$$\left(\frac{mA}{j\,cm2}\right)\left(\frac{1A}{1000\,mA}\right)\left(\frac{1C/s}{1A}\right)\left(\frac{1\ mol\ e-}{96485.3\ C}\right)\left(\frac{1\ mol\ H2}{2\ mol\ e-}\right) \times \left(\frac{6.022 \times 10\ 23\ molecules}{1\ mol\ H2}\right) H_2) = 3.12 \times 10^{15}\ \frac{H2/s}{cm2}\ \text{per}\ \frac{mA}{cm2}$$

The current density at an overpotential of 100 mV in 1 M KOH is 71.86 mA cm^{-2}; therefore, the TOF per site is calculated as,

$$\frac{\left(3.12 \times 1015\ \frac{H2/s}{cm2}\ per\ \frac{mA}{cm2}\right)\left(71.86\ \frac{mA}{cm2}\right)}{3.06 \times 1017} = 0.733\ \frac{H2/s}{surface\ site}$$

The TOFs of CoPB/NF and ZIF-67/NF were calculated in the same manner as those of CoPB@ZIF-67/NF electrode methods:

CoPB/NF catalyst: TOF = $0.244\ \frac{H2/s}{surface\ site}$

ZIF-67/NF catalyst: TOF = $0.157\ \frac{H2/s}{surface\ site}$

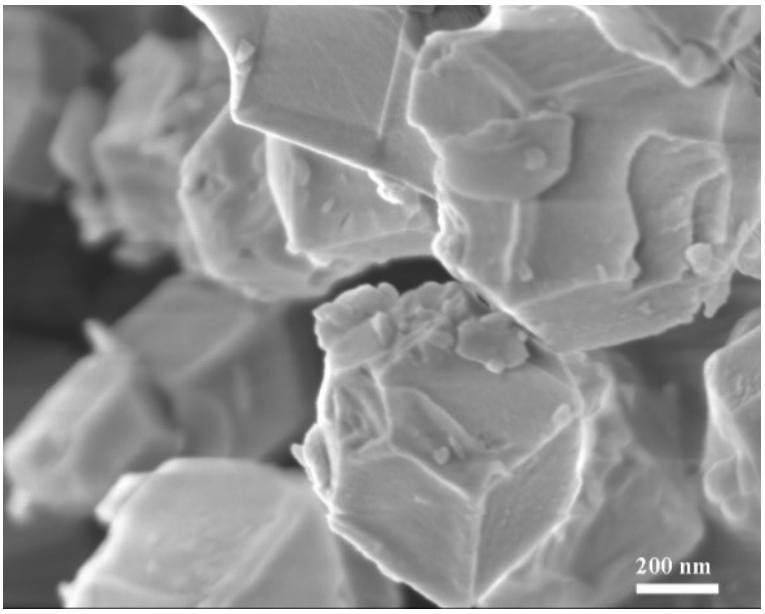

Fig. S1. Field-emission scanning electron microscopy **(**FESEM) images of ZIF-67.

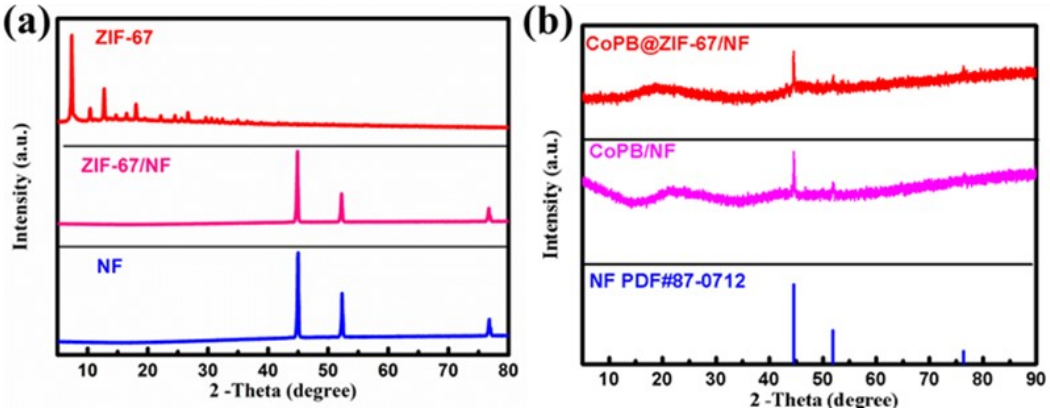

Fig. S2. XRD pattern of catalyst (a) NF, ZIF-67 and ZIF-67/NF. (b) CoPB@ZIF-67/NF, CoPB/NF and PDF#87-0712.

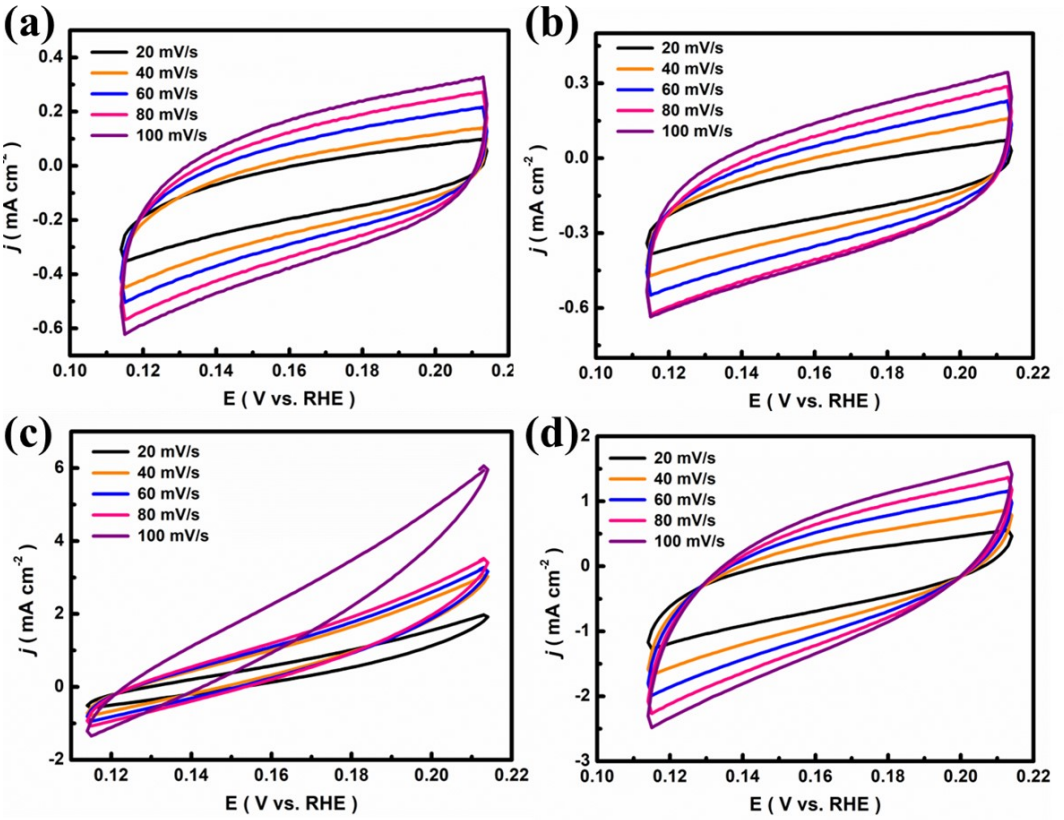

Fig. S3. CV curves of (a) Nickel foam, (b) ZIF-67/NF, (c) CoPB/NF, (d) CoPB@ZIF-67/NF at different scan rates (20 to 100 mV s^{-1}) for HER.

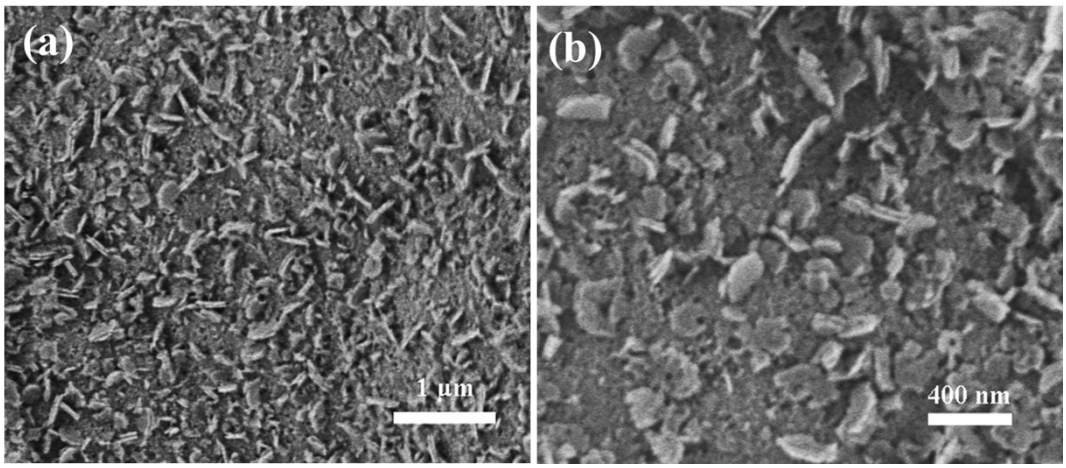

Fig. S4. FESEM images of CoPB@ZIF-67/NF after chronopotentiometry test for 100 h at 10 mA cm^{-2}.

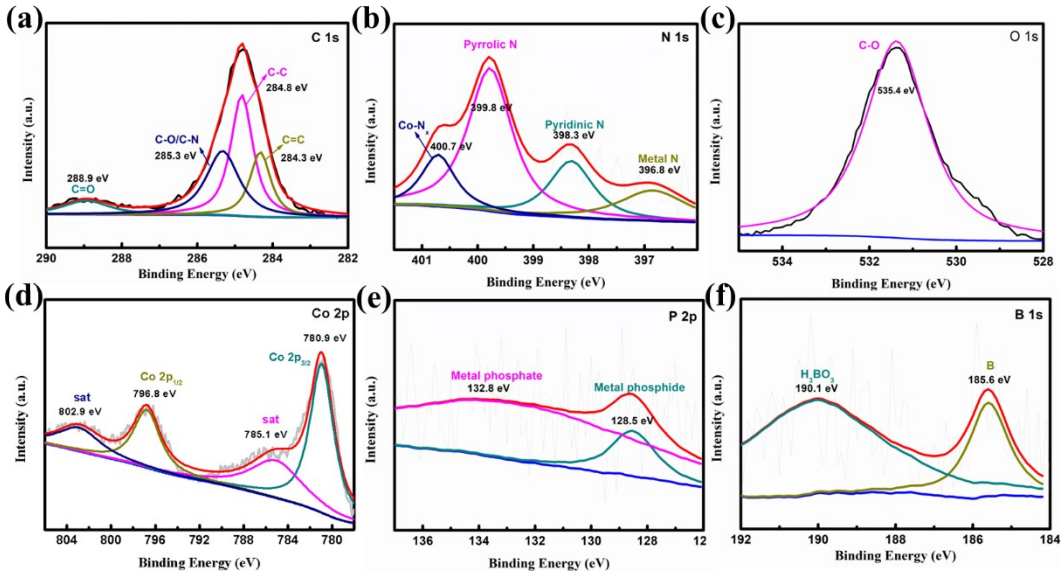

Fig. S5. High-resolution XPS spectra of (a) C 1s, (b) N 1s, (c) O 1s, (d) Co 2p, (e) P 2p and (f) B 1s for CoPB@ZIF-67/NF after chronopotentiometry test for 100 h at 10 mA cm^{-2}.

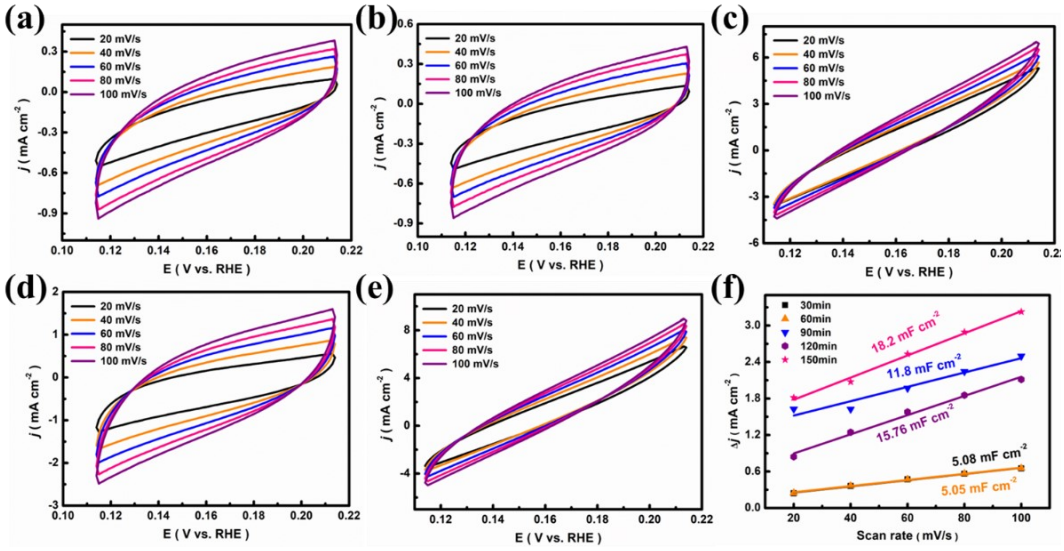

Fig. S6. CV curves and C_{dl} value of CoPB@ZIF-67/NF at different reaction times at different scan rates (20 to 100 mV s^{-1}) for HER. (a-e) 30 min, 60 min, 90 min, 120 min, 150 min. (f) C_{dl} value.

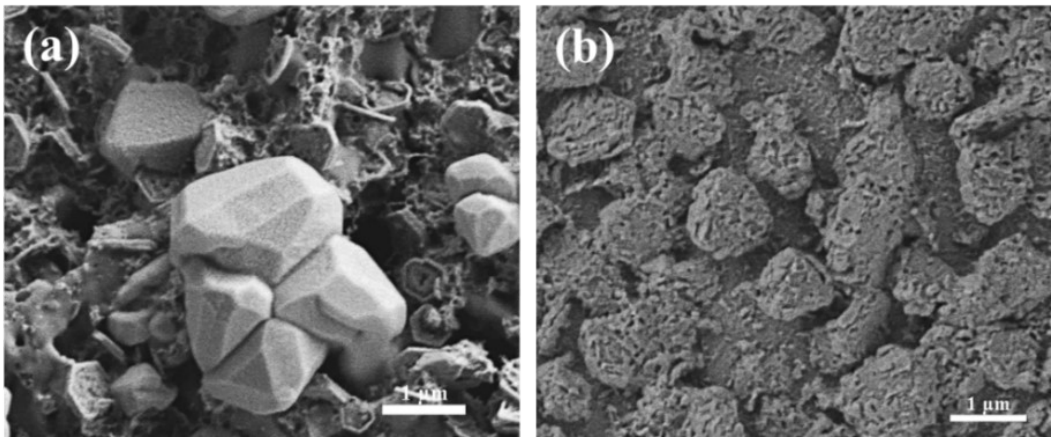

Fig. S7. FESEM images of catalyst (a) CoP@ZIF-67/NF, (b) CoB@ZIF-67/NF.

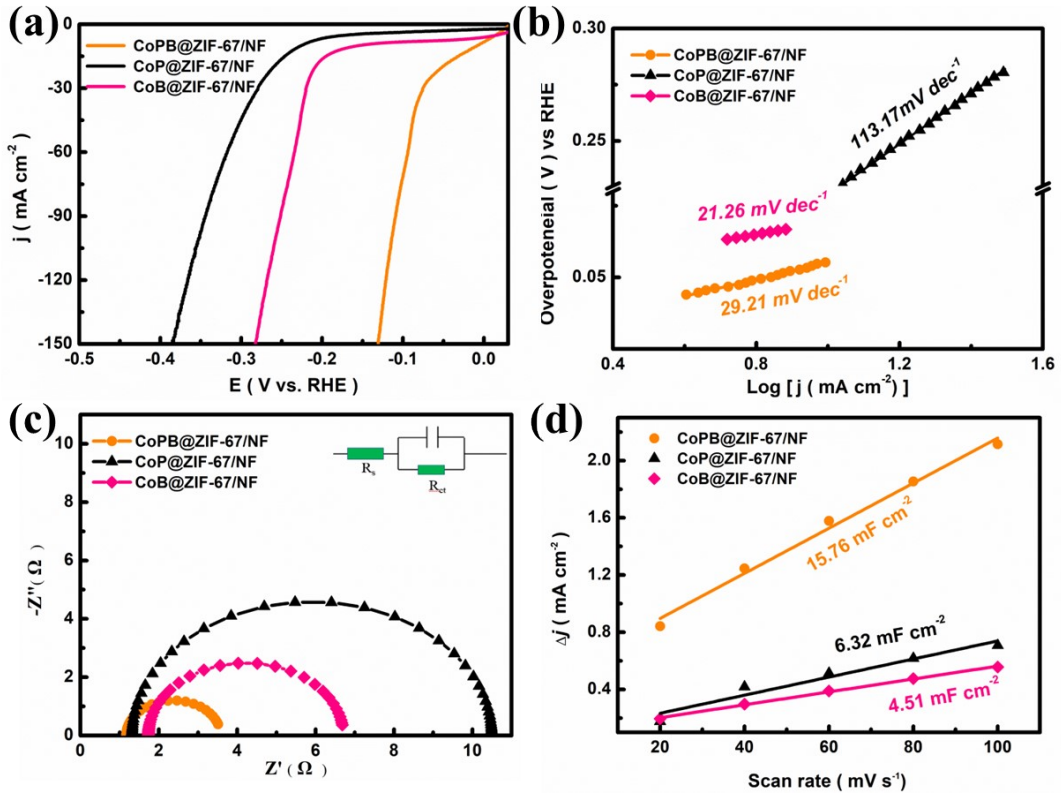

Fig. S8. CoPB@ZIF-67/NF, CoP@ZIF-67/NF, CoB/NF and CoPB@ZIF-67/NF (a) iR-corrected LSV polarization curves. (b) Tafel slope plots. (c) Nyquist plots (inset: the fitted circuit diagram). (d) C_{dl} value.

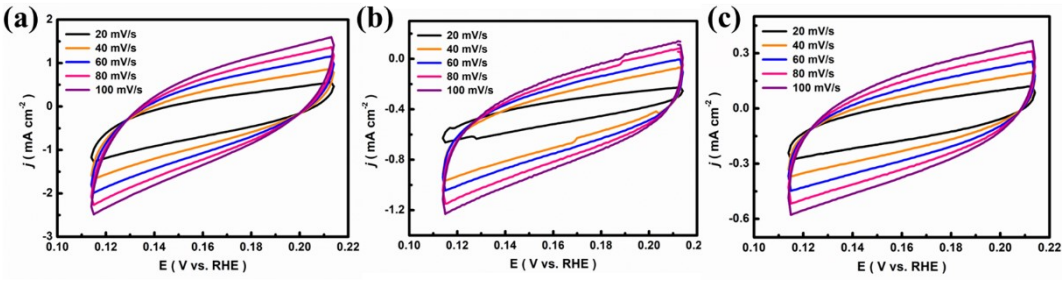

Fig. S9. CV curves of (a) CoPB@ZIF-67/NF, (b) CoP@ZIF-67/NF and (c) CoB@ZIF-67/NF at different scan rates (20 to 100 mV s^{-1}) for HER.

Table S1. ICP-OES results of CoPB@ZIF-67/NF catalyst

Sample	Co (wt%)	P (wt%)	B (wt%)
CoPB@ZIF-67/NF	70.3	1.07	0.18

Table S2. The performance of different catalysts for HER in 1 M KOH

catalysts	η_{10} (mV)	η_{50} (mV)	η_{100} (mV)	Tafel plot (mV dec^{-1})
NF	244	332	385	117.17
Pt-C/NF	26	86	127	79.72
ZIF-67/NF	204	310	351	131.02
CoPB/NF	66	175	226	53.36
CoPB@ZIF-67/NF	9	90	114	29.21
CoP@ZIF-67/NF	227	306	352	113.17
CoB@ZIF-67/NF	155	229	257	21.26

Note: η_{10} is the overpotential at a current density of 10 mA cm^{-2}, η_{50} is the overpotential at a current density of 50 mA cm^{-2}, η_{100} is the overpotential at a current density of 100 mA cm^{-2}

Table S3. Comparison of hydrogen evolution performance of heterogeneous catalysts

Catalysts	Electrolyte	j = 10 mA cm^{-2}		Ref
		Overpotential (mV)	Tafel plot (mV dec^{-1})	
CoPB@ZIF-67/NF	1 M KOH	9	29.21	This work
Co_2P/Co_4N	1 M KOH	40	56	1
MoS_2–MoP/C	1 M KOH	102	58	2
Co–MoC/Mo_2C-0.5	1 M KOH	82	54	3
Ni/NiFe-LDO/NF	1 M KOH	29	82	4
MoS_2-MoO_{3-x}/Ni_3S_2@NF	1 M KOH	76	53.2	5
RuO_2/RuP_2/Ru	1 M KOH	33	36.7	6

W-NiS_2/MoO_2@CC	1 M KOH	52	49	7
$Co_2N_{0.67}$/MoO_2/MF	1 M KOH	75.2	150.3	8
Ni_3P-Ni/CNT	1 M KOH	116	59	9
CoP–MoO_2/MF	1 M KOH	42	127	10
Mo_2N/Mo_2C	1 M KOH	88.1	68.5	11
Fe–Co–P/NF	1 M KOH	87	63	12
Zn-VO_x-Co	1 M KOH	46	75	13
Au/Ni_3S_2/NF	1 M KOH	97	72	14
Ni_2P@MoS_2/CC	1 M KOH	99	97	[15]

Table S4. Consists of elements of CoPB@ZIF-67/NF determined by XPS before and after stability test

Sample	C (at%)	N (at%)	O (at%)	Co (at%)	P (at%)	B (at%)
Before stability test	51.47	3.91	24.5	6.19	1.54	12.4
After stability test	42.64	2.93	34.31	10.38	2.58	7.16

References

1 Y. Men, S. Jia, P. Li, Y. Tan, J. Wang, P. Zhao, G. Cheng, S. Chen, W. Luo, Boosting alkaline hydrogen evolution electrocatalysis through electronic communicating vessels on Co_2P/Co_4N heterostructure catalyst, *Chem. Eng. J.*, 2022, **433**, 133831.

2 Z. Wu, J. Wang, K. Xia, W. Lei, X. Liu, D. Wang, MoS_2–MoP heterostructured nanosheets on polymer-derived carbon as an electrocatalyst for hydrogen evolution reaction, *J. Mater. Chem. A*, 2018, **6**, 616-622.

3 J. Li, R. Ge, P. Lan, J. Yang, J. Feng, Y. Li, S. Li, B. Liu, W. Li, In situ phase transition induced TM–MoC/Mo_2C (TM= Fe, Co, Ni, and Cu) heterostructure catalysts for efficient hydrogen evolution, *J. Mater. Chem. A*, 2022, **10**, 10493-10502.

4 Y. Tian, A. Huang, Z. Wang, M. Wang, Q. Wu, Y. Shen, Q. Zhu, Y. Fu, M. Wen, Two-dimensional hetero-nanostructured electrocatalyst of Ni/NiFe-layered double oxide for highly efficient hydrogen evolution reaction in alkaline medium, *Chem. Eng. J.*, 2021, **426**, 131827.

5 M. Luo, S. Liu, W. Zhu, G. Ye, J. Wang, Z. He, An electrodeposited MoS_2-MoO_{3-x}/Ni_3S_2 heterostructure electrocatalyst for efficient alkaline hydrogen evolution, *Chem. Eng. J.*, 2022, **428**, 131055.

6 Y. Zhao, X. Zhang, Y. Gao, Z. Chen, Z. Li, T. Ma, Z. Wu, L. Wang, S. Feng, Heterostructure of RuO_2-RuP_2/Ru Derived from HMT-based Coordination Polymers as Superior pH-Universal Electrocatalyst for Hydrogen Evolution Reaction, *Small*, 2022, **18**, 2105168.

7 S. Ligani Fereja, P. Li, Z. Zhang, J. Guo, Z. Fang, Z. Li, S. He, W. Chen, W-doping induced abundant active sites in a 3D NiS_2/MoO_2 heterostructure as an efficient electrocatalyst for urea oxidation and hydrogen evolution reaction, *Chem. Eng. J.,* 2022, **432**, 134274.

8 R. Tong, M. Xu, H. Huang, C. Zhang, Y. Ma, X. Wang, X. Hu, Y. Qu, S. Wang, H. Pan, $Co_2N_{0.67}$/MoO_2 Heterostructure as High-Efficiency Electrocatalysts for the Hydrogen Evolution Reaction, *ACS Appl. Energy Mater.*, 2022, **5**, 440-448.

9 D. Li, Z.-F. Zhang, Z.-Y. Yang, W.-Y. Wu, M.-H. Zhang, T.-R. Yang, Q.-S. Zhang, J.-Y. Xie, Ni_3P-Ni heterostructure electrocatalyst for alkaline hydrogen evolution, *J. Alloys Compd.*, 2022, **921**, 166204.

10 H. Zhao, Z. Li, X. Dai, M. Cui, F. Nie, X. Zhang, Z. Ren, Z. Yang, Y. Gan, X.

Yin, Y. Wang, W. Song, Heterostructured CoP/MoO_2 on Mo foil as high-efficiency electrocatalysts for the hydrogen evolution reaction in both acidic and alkaline media, *J. Mater. Chem. A*, 2020, **8**, 6732-6739.

11 B. Zhang, H. Xu, Q. Chen, H. Chen, G. He, ZIF-67 derived Mo_2N/Mo_2C heterostructure as high-efficiency electrocatalyst for hydrogen evolution reaction, *J. Alloys Compd.*, 2022, **922**, 166216.

12 H. Xu, J. Zhu, P. Wang, D. Chen, C. Zhang, M. Xiao, Q. Ma, H. Bai, R. Qin, J. Ma, S. Mu, Fe–Co–P multi-heterostructure arrays for efficient electrocatalytic water splitting, *J. Mater. Chem. A*, 2021, **9**, 24677-24685.

13 M. Chen, J. Liu, N. Kitiphatpiboon, X. Li, J. Wang, X. Hao, A. Abudula, Y. Ma, G. Guan, Zn-VO_x-Co nanosheets with amorphous/crystalline heterostructure for highly efficient hydrogen evolution reaction, *Chem. Eng. J.*, 2022, **432**, 134329.

14 H. Liu, J. Cheng, W. He, Y. Li, J. Mao, X. Zheng, C. Chen, C. Cui, Q. Hao, Interfacial electronic modulation of Ni_3S_2 nanosheet arrays decorated with Au nanoparticles boosts overall water splitting, *Appl. Catal. B Environ.*, 2022, **304**, 120935.

15 Y. Dai, W. Chen, B. Guo, X. Li, J. Guan, L. Wang, M. Zhang, $Ni_2P@MoS_2$/CC catalysts with heterogeneous structure are used for highly efficient electrolysis of water for hydrogen evolution, *J. Mater. Chem. A*, 2022, **905**, 164157.